Processing and Application of Ceramics 17 [3] (2023) 314–320
https://doi.org/10.2298/PAC2303314N

Mechanical and electronic properties of $NiCo_2O_4$ under high pressure – A first-principles calculation

Veerappan Nagarajan[1], Karthigayan Padmashri[2], Ramanathan Chandiramouli[1,*]

[1]*School of Electrical & Electronics Engineering, SASTRA Deemed University, Tirumalaisamudram, Thanjavur - 613 401, India*
[2]*School of Mechanical Engineering, SASTRA Deemed University, Tirumalaisamudram, Thanjavur - 613 401, India*

Received 30 January 2023; Received in revised form 6 July 2023; Accepted 30 August 2023

Abstract

The mechanical and electronic properties of $NiCo_2O_4$ crystal under high pressure are explored based on the density functional theory method. The pressure in the range from 0 to 50 GPa is applied to $NiCo_2O_4$ and the behaviour concerning electronic properties is studied. The energy band gap of $NiCo_2O_4$ gradually decreases from 2.196 eV (0 GPa) to 1.785 eV (50 GPa). The elastic constants for cubic $NiCo_2O_4$ are calculated and bulk, shear and Young's modulus are further computed. Furthermore, Cauchy's pressure, Pugh's criterion and Poisson's ratio of $NiCo_2O_4$ are calculated and reported under high pressure. The $NiCo_2O_4$ exhibits ductile property under high pressure, which is evident from Pugh's criterion. In addition, hardness and anisotropy factor is also calculated and reported.

Keywords: *$NiCo_2O_4$, high pressure, Pugh's criterion, hardness, energy gap*

I. Introduction

Oxides constitute a major class of materials that find their potential importance as catalysts, chemical sensors, biosensors and energy materials [1]. Besides, metal oxide nanopowders are used in microwave absorption devices, electronic devices and chemical nanosensors [2]. Moreover, all electrochemical, magnetic, electrical and catalytic properties of nanostructured metal oxides are influenced by their morphology, structure, size and chemical composition [3]. Nickel cobaltite ($NiCo_2O_4$) is one of the broadly used and immensely popular spinel-structured metal oxides, which finds its potential importance in supercapacitors [4]. It has the generic formula AB_2O_4, which exhibits a spinel structure. Besides, $NiCo_2O_4$ with the general formula AB_2O_4 is considered to be a cubic spinel structure [5]. The cations A and B are organized in tetrahedral and octahedral sites partially with oxygen atoms spread in a cubic close-packed structure [5]. In the case of the inverse spinel structure of $NiCo_2O_4$, half of the Co ions occupies the tetrahedral sites (A sites) and the other half of Co atoms and all Ni atoms occupies octahedral sites (B sites) [6]. Spinel oxide nanostructures of general formula AB_2O_4 are known to be potential energy storage materials [7].

$NiCo_2O_4$ has become immensely popular due to its cost-effectiveness, diverse valence state, environmental friendliness, high specific capacitance and electrochemical active sites [8]. Li *et al.* [9] studied the electromagnetic wave absorption features of $NiCo_2O_4$ prepared by hydrothermal process. Moreover, 3D multilayer flower-like $NiCo_2O_4$ prepared with a calcination temperature of 400 °C exhibits excellent electromagnetic wave absorption characteristics [9]. Besides, $NiCo_2O_4$ is widely used as supercapacitors, photocatalysis, magnetic devices and in H_2O_2 reduction reactions [10]. Guo *et al.* [6] synthesized $NiCo_2O_4$ films at a lower temperature ($T < 450$ °C) which exhibit ferrimagnetic properties. Raja *et al.* [11] synthesised $NiCo_2O_4$ nanosheets using the hydrothermal method with a large surface area for high-performance asymmetric supercapacitors. $NiCo_2O_4$ prepared by the solvothermal process was reported by Sethi *et al.* [12], which was used in supercapacitors. Furthermore, hydrothermal, microwave-assisted, solvothermal, sol-gel approaches, coprecipita-

* Corresponding author: tel: +91 948 9566466,
e-mail: *rcmoulii@gmail.com*

tion and thermal decomposition are the most common ways of synthesizing transition metal oxides. Ferrimagnetic cubic spinel structure with good electrical conductivity and multiple redox sites has been observed in p-type semiconductor $NiCo_2O_4$ with an optical band gap of 2.1 eV in which cobalt cations reside along the tetrahedral and octahedral interstitial sites and nickel cation in the octahedral sites [5]. Zhu *et al.* [13] reported that spinel oxide nanostructures like $NiCo_2O_4$ are used as potential energy storage materials owing to their better chemical performances, achievable oxidation states and high electrical conductivity. Besides, redox reactions from both Co and Ni ions bring high specific capacitance for the $NiCo_2O_4$ electrode. [13]. The high electronic conductivity of $NiCo_2O_4$ is necessary for fast electron transfer in electrochemical reactions. It also favours the electrocatalytic activity which is also due to the mixed valence state of the spinel structure. These can be further enhanced by modifying the morphology of urchin and sheaf-like nanostructures of $NiCo_2O_4$ [14]. Tomboc *et al.* [15] has reported that $NiCo_2O_4$ can be used as a substitute for Pt-free electrocatalysts for direct methanol fuel cells owing to its excellent corrosion stability in alkaline solution and higher electronic conductivity. The three-dimensional hierarchical structure of $NiCo_2O_4$ and the mesoporous surface has more electro-active for electrochemical reactions. It helps in the conduction of electrolyte ions which increases the electrochemical activity of the materials [15].

In the current work, $NiCo_2O_4$ structure is studied under high pressure ranging from 0 up to 50 GPa and the electronic and mechanical properties are reported. The motivation of the present work is to fine-tune the mechanical as well as the electronic properties of $NiCo_2O_4$ under high pressure and to check the suitability of $NiCo_2O_4$ as a pressure sensor.

II. Computational specifications

The first-principles calculations on $NiCo_2O_4$ crystal are studied based on the density functional theory (DFT) method using Quantum-Atomistic Toolkit (ATK) package [16]. The $NiCo_2O_4$ structures are studied utilizing the generalized gradient approximation within the framework of the B3LYP level of theory [17,18]. The Brillouin zone of $NiCo_2O_4$ is sampled with a Monkhorst-Pack grid of $12 \times 12 \times 12$ k-points. The double zeta polarization basis set is employed during the relaxation of $NiCo_2O_4$ in the current work [19,20]. The energy cut off was kept at 500 eV and the energy convergence is maintained at 10^{-6} eV. The atomic positions of $NiCo_2O_4$ were optimized until the force of 0.003 eV/Å achieved.

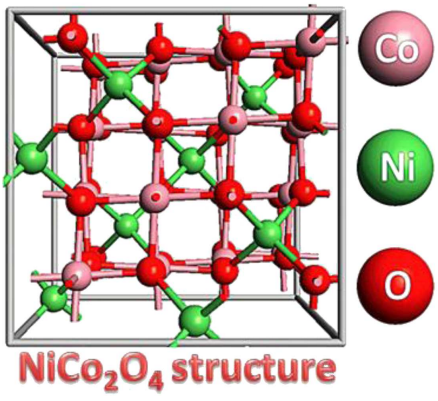

Figure 1. Illustration of $NiCo_2O_4$ structure

III. Results and discussion

3.1. Band structure of $NiCo_2O_4$ at high pressure

The structure of $NiCo_2O_4$ possesses a space group of $Fd\bar{3}m$. As we mentioned above that the proposed $NiCo_2O_4$ belongs to a cubic spinel structure with general formula AB_2O_4 in which the cations A and B are located partially in octahedral and tetrahedral sites along with distributed oxygen atoms in close-packed cubic structure as shown in Fig. 1. The optimized lattice parameters of the proposed $NiCo_2O_4$ cubic structure are found to be $a = b = c = 8.21$ Å. The bond length between Ni–O and Co–O is calculated to be 1.927 Å each. The obtained lattice parameter in the present work is consistent with the former computational report [21]. In the present work, the elastic properties of $NiCo_2O_4$ are calculated [22]. Initially, we studied the electronic and mechanical properties of cubic $NiCo_2O_4$ at 0 GPa. Figure 1 represents the illustration of $NiCo_2O_4$. Subsequently, $NiCo_2O_4$ is subjected to high pressures of 10, 20, 30, 40 and 50 GPa, and their changes in the electronic and mechanical properties are explored.

Figure 2 represents the band structure of $NiCo_2O_4$ at different pressures. The insights on the energy band gap of $NiCo_2O_4$ are ascertained based on the energy band structure [23–27]. At 0 GPa, it is observed that the energy band gap is 2.196 eV along the gamma point. The obtained band gap is in accordance with the previously reported experimental value of 2.32 eV [28]. Chang *et al.* [29] reported the band gap of $NiCo_2O_4$ as 0.9 eV using the GGA/PBE level of theory. In the present work, we use the hybrid-GGA/B3LYP level of theory to calculate the band gap to avoid the underestimation issue. Interestingly, on increasing the pressure, the energy band gap of $NiCo_2O_4$ decreases gradually and it reaches 1.785 eV at 50 GPa. Moreover, on applying pressure to $NiCo_2O_4$, the small vibration occurs in the crystal lattice leading to slight variation in the lattice constant. The variation in lattice constant leads to the variation in the band gap [30]. Furthermore, the band gap variation is found to be less upon applying pressure to $NiCo_2O_4$, which infers that the lattice distortion does not happen up to 50 GPa.

3.2. Elastic constants of cubic $NiCo_2O_4$

The examination of elastic constants gives in-depth information with regard to mechanical stability, chemi-

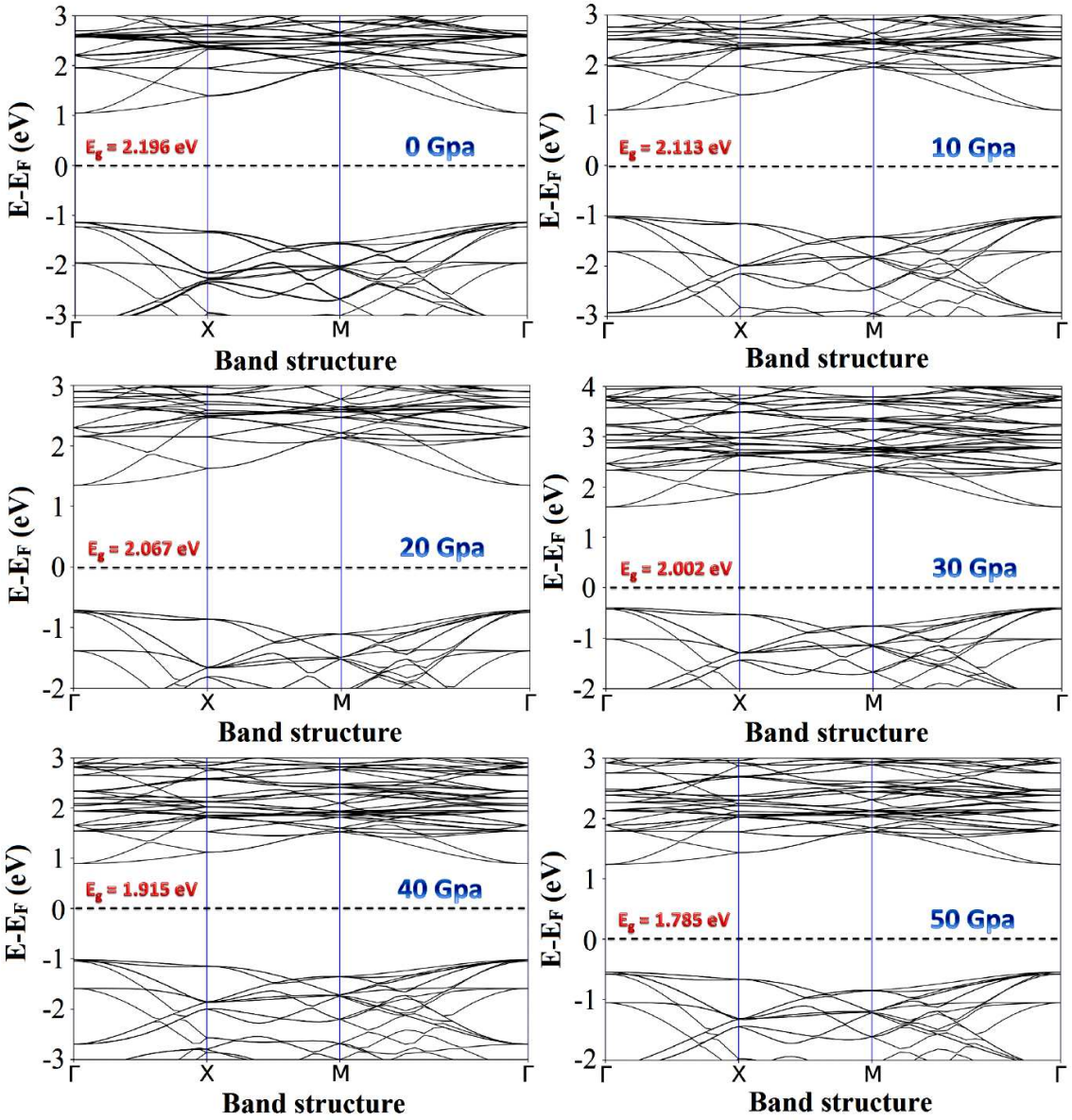

Figure 2. Band structure of $NiCo_2O_4$ at different pressures from 0 to 50 GPa

cal bond and electronic and mechanical properties [31–33]. Moreover, the properties such as anisotropy, ductility, brittleness and stability of $NiCo_2O_4$ crystal can be explored with the help of elastic constants. Table 1 depicts the elastic constants of cubic $NiCo_2O_4$ crystal at different pressures. The elastic constant C_{11}, C_{12} and C_{44} for a cubic structure and the Born stability criterion are given as follows:

$$C_{11} - C_{12} > 0,\ C_{11} + 2C_{12} > 0,\ C_{44} > 0 \qquad (1)$$

From Table 1 it can be revealed that $NiCo_2O_4$ structure is mechanically stable based on the Born stability criterion.

Table 1. Elastic constants of cubic $NiCo_2O_4$ structure at different pressures

Pressure [GPa]	C_{11}	C_{12}	C_{44}
0	138.92	87.19	79.90
10	193.58	111.36	90.09
20	222.97	140.98	100.22
30	291.50	178.67	111.40
40	348.43	212.61	121.26
50	391.28	247.17	129.61

3.3. Mechanical properties of cubic $NiCo_2O_4$

The Voigt-Reuss-Hill averaging schemes are used to analyze the mechanical properties of $NiCo_2O_4$ [34,35].

The Reuss and Voigt bulk (B_R, B_V) and shear modulus (G_R, G_V) are given as:

$$B_V = B_H = \frac{C_{11} + 2C_{12}}{3} \qquad (2)$$

$$G_V = \frac{C_{11} - C_{12} + 3C_{44}}{5} \qquad (3)$$

Table 2. Bulk (B), shear (G) and Young's modulus (E) of $NiCo_2O_4$ structure under high pressure

Pressure [GPa]	B_R	B_V	B_H	G_R	G_V	G_H	E_R	E_V	E_H
0	104.43	104.43	104.43	43.53	58.29	50.91	71.68	71.68	71.68
10	138.76	138.76	138.76	61.01	70.50	65.76	112.24	112.24	112.24
20	168.31	168.31	168.31	63.52	76.53	70.02	113.76	113.76	113.76
30	216.28	216.28	216.28	80.15	89.41	84.78	155.71	155.71	155.71
40	257.88	257.88	257.88	92.26	99.92	96.09	187.28	187.28	187.28
50	295.21	295.21	295.21	98.23	106.59	102.41	199.91	199.91	199.91

$$G_R = \frac{5C_{44}(C_{11} - C_{12})}{4C_{44} + 3(C_{11} - C_{12})} \tag{4}$$

Hill bulk and shear moduli are given by the following formulas:

$$B_H = \frac{B_V + B_R}{2} \tag{5}$$

$$G_H = \frac{G_V + G_R}{2} \tag{6}$$

Young's modulus (E) and Poisson's ratio (ν) are given by the following relations:

$$E = \frac{9B \cdot G}{3B + G} \tag{7}$$

$$\nu = \frac{3B - 2G}{2(3B + G)} \tag{8}$$

Bulk modulus (B) gives the measurement of volume detention whereas shear modulus (G) gives the material's impedance to reversible deformation [36]. Young's modulus gives the ductility and stiffness measurement of materials. The shear modulus, Young's modulus and bulk modulus of $NiCo_2O_4$ structure at varied pressure till 50 GPa are presented in Table 2.

It is observed that the values of shear modulus, Bulk modulus and Young's modulus increase with the increase in pressure. Voigt-Reuss-Hill bulk modulus and Young's modulus are the same at all varied pressures but differences are noticed in shear modulus, nonetheless, the trend is increasing with an increase in pressure. It is well known that the hardness of $NiCo_2O_4$ depends on the shear modulus. The large value of shear modulus for increasing temperature indicates the ductile nature of $NiCo_2O_4$ under high pressure [37]. To understand the brittleness and ductility of a material, the required mechanical characteristic is Pugh's criterion (B/G) [38].

At 0 GPa, Pugh's criterion value of $NiCo_2O_4$ is 2.400 (Table 3). It is observed that Pugh's criterion increases remarkably on increasing the pressure to 50 GPa. It is a known fact that if $(B/G) > 1.75$, the material possesses ductile nature [38]. The first, on applying 10 GPa pressure, Pugh's criterion decreases to a value of 2.274, and increasing the pressure up to 50 GPa, the ductility of $NiCo_2O_4$ also escalates. It can be inferred that the valence electrons in $NiCo_2O_4$ get delocalised which allows the atoms to slide easily. This happens effortlessly and efficiently as the pressure increases and therefore

Table 3. Pugh's criterion and Poisson's ratio for $NiCo_2O_4$ structure under high pressure

Pressure [GPa]	Pugh's criterion (B/G)	Poisson's ratio (ν)
0	2.400	0.386
10	2.274	0.365
20	2.650	0.387
30	2.698	0.380
40	2.795	0.379
50	3.005	0.387

the ductile nature increases. To understand the plasticity and how deformation occurs in the lateral direction with respect to the axial direction, we should know the values of Poisson's ratio (ν). For $NiCo_2O_4$ at 0 GPa ν = 0.386. On applying 10 GPa, the value of ν drops to 0.365, which indicates that there is a deformation on applying the pressure. Moreover, for a pressure of 20 GPa, the value of ν is increased to 0.387. Further, ν does not increase for the applied pressure from 30 to 50 GPa. For 50 GPa, the value increases to 0.387. When Poisson's ratio is higher than 0.26 it refers to good ductility, in contrast, the low value indicates the brittle nature [39]. Besides, the Poisson's ratio calculated for $NiCo_2O_4$ under pressure ranges from 0.365 to 0.387, which indicates the ductile nature of $NiCo_2O_4$ upon applied pressure. The larger values of ν refer to large elastic deformation compared to other values.

Hardness refers to the resistance against deformation and it is given by the following equation [39–41]:

$$H_V = 0.92K^{1.137}G^{0.708} \tag{9}$$

where $K = G/B$. The hardness of $NiCo_2O_4$ at 0 GPa is 4.919 GPa (Table 4). On increasing the pressure, the calculated results show that the hardness increases and decreases at varied pressure. Besides, the maximum hardness obtained at 40 GPa is 7.038 GPa. At first on applying 10 GPa, the hardness increases to 6.631 GPa. It is observed from the graph as illustrated in Fig. 3 that Cauchy's pressure ($C_{12} - C_{44}$) increases proportionately with increasing pressure. These variations of Cauchy's pressure with an increase in variations reflect the nature of the bonding at the atomic level. The universal anisotropic index (A^U) is given by the expression [42,43]:

$$A^U = \frac{5G_V}{G_R} + \frac{B_V}{B_R} - 6 \geq 0 \tag{10}$$

Table 4. Hardness value of $NiCo_2O_4$ nanostructure under high pressure

Pressure [GPa]	Hardness [GPa]
0	4.919
10	6.639
20	5.742
30	6.631
40	7.038
50	6.775

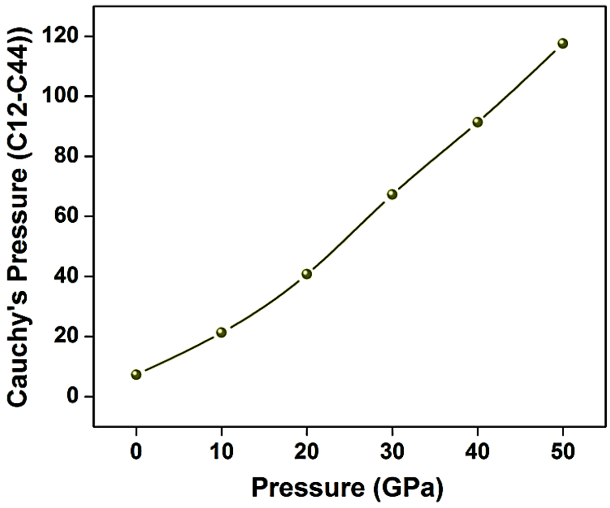

Figure 3. Illustration of Cauchy's pressure plot

Figure 4 illustrates the pressure versus anisotropy factor plot. Moreover, it is known that for isotropic materials A^U is 0. However, a larger value of A^U refers to the greater anisotropy of the material. Besides, the A^U values for $NiCo_2O_4$ were found to vary from 0 to 50 GPa. Using A^U we can study the microcracks of the proposed material and it can be related to nanoscale precursor textures. Since the anisotropy of the material mainly varies with respect to the degree of deviation from 0 to 50 GPa. We can also compare the anisotropy with the hardness of the material. The higher

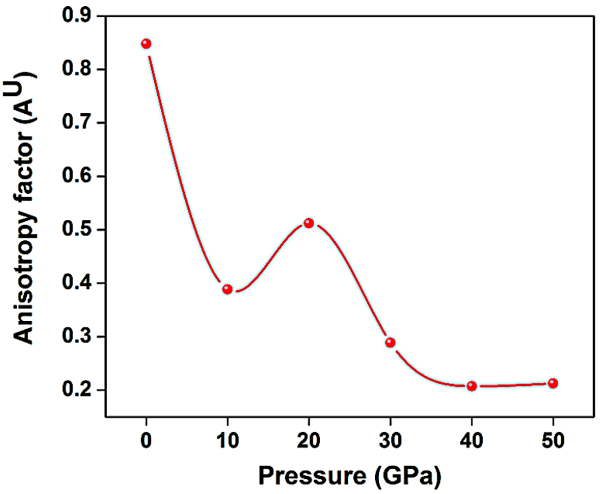

Figure 4. Pressure versus anisotropy factor plot

the hardness, the smaller anisotropy is observed [30]. The anisotropy index of $NiCo_2O_4$ is found to be highest at 0 GPa. Nonetheless, for 10 GPa, there is a large drop in the A^U. At 20 GPa, there is a small increase in the value of A^U and further increasing the pressure till 50 GPa, the value of A^U decreases remarkably. Thus, it is inferred that $NiCo_2O_4$ crystal possesses different chemical and physical properties in different directions owing to its anisotropic properties [41].

IV. Conclusions

To sum up, the mechanical and electronic properties of $NiCo_2O_4$ are studied using the DFT method upon varying the pressure from 0 up to 50 GPa. The elastic constants of cubic $NiCo_2O_4$ are calculated initially. Furthermore, the elastic constants are used to compute bulk, shear and Young's modulus of $NiCo_2O_4$ under various pressures. Besides, Pugh's criterion and Poisson's ratio of $NiCo_2O_4$ show that under high pressure, $NiCo_2O_4$ exhibits ductile-like properties. The Cauchy's pressure, hardness and anisotropy factor of $NiCo_2O_4$ are calculated under high pressure. The hardness of $NiCo_2O_4$ increases upon an increase in pressure. The electronic properties of $NiCo_2O_4$ under pressure are studied based on the energy band structure diagrams. Moreover, the energy gap gradually decreases from 2.196 eV to 1.785 eV upon increasing pressure from 0 to 50 GPa. Thus, the proposed study gives insights into the electronic and mechanical properties of $NiCo_2O_4$ structure under various pressures, where the energy band gap and mechanical properties of $NiCo_2O_4$ can be tailored for various engineering applications.

Acknowledgement: The authors wish to express their sincere thanks to FIST funding (SR/FST/PS-1/2020/135), DST-SERB funding (CRG/2022/001954) for financial support.

References

1. G. Marimuthu, G. Palanisamy, T. Pazhanivel, G. Bharathi, M.M. Cristopher, K. Jeyadheepan, "Nanorod like $NiCo_2O_4$ nanostructure for high sensitive and selective ammonia gas sensor", *J. Mater. Sci. Mater. Electron*, **31** (2019) 1951–1959.
2. Y. Yoon, P.L. Truong, D. Lee, S.H. Ko, "Metal-oxide nanomaterials synthesis and applications in flexible and wearable sensors", *ACS Nanosci. Au*, **2** (2021) 64–92.
3. M.S. Chavali, M.P. Nikolova, "Metal oxide nanoparticles and their applications in nanotechnology", *SN Appl. Sci.*, **1** (2019) 607.
4. C.-C. Yang, W.-C. Sun, A. Kumar, B. Pattanayak, T.-Y. Tseng, "Templating synthesis of nickel cobaltite nanoflakes and their nanocomposites for making high-performance symmetric supercapacitors", *Mater. Today Energy*, **14** (2019) 100356.
5. S. Karmakar, S. Varma, D. Behera, "Investigation of structural and electrical transport properties of nano-flower shaped $NiCo_2O_4$ supercapacitor electrode materials", *J. Alloys Compd.*, **757** (2018) 49–59.

6. W. Guo, C. Zhen, C. Wu, X. Wu, G. Li, L. Ma, D. Hou, "Influence of growth temperature on the microstructure and electrical transport properties of epitaxial $NiCo_2O_4$ thin films", *Ceram. Int*., **44** (2018) 12539–12546.
7. J.A. Rajesh, B.-K. Min, J.-H. Kim, H. Kim, K.-S. Ahn, "Cubic spinel AB_2O_4 type porous $ZnCo_2O_4$ microspheres: Facile hydrothermal synthesis and their electrochemical performances in pseudocapacitor", *J. Electrochem. Soc.*, **163** (2016) A2418–A2427.
8. X.-F. Zhang, X.-H. Zuo, W.-J. Zhu, P.-L. Che, D.-W. Shi, S.-S. Chen, "Morphology and electrochemical properties of $NiCo_2O_4$ powders prepared by a facile hydrothermal method", *Ceram. Int*., **48** (2022) 20984–20995.
9. K. Li, Y. Shen, L. Xu, H. Pan, N. Shen, H. Ling, K. Ni, Z. Ni, G. Xiang, "Achieving electromagnetic wave absorption capabilities by fabrication of flower-like structure $NiCo_2O_4$ derived from low-temperature co-precipitation", *Vacuum*, **205** (2022) 111493.
10. X. Yang, X. Yu, Q. Yang, D. Zhao, K. Zhang, J. Yao, G. Li, H. Zhou, X. Zuo, "Controllable synthesis and magnetic properties of hydrothermally synthesized $NiCo_2O_4$ nanospheres", *Ceram. Int*., **43** (2017) 8585–8589.
11. R. BoopathiRaja, M. Parthibavarman, "Reagent induced formation of $NiCo_2O_4$ with different morphologies with large surface area for high performance asymmetric supercapacitors", *Chem. Phys. Lett*., **755** (2020) 137809.
12. M. Sethi, D.K. Bhat, "Facile solvothermal synthesis and high supercapacitor performance of $NiCo_2O_4$ nanorods", *J. Alloys Compd*., **781** (2019) 1013–1020.
13. Y. Zhu, J. Chen, N. Zhao, W. Lin, C. Lai, Q. Wang, "Large-scale synthesis of uniform $NiCo_2O_4$ nanoparticles with supercapacitive properties", *Mater. Lett*., **160** (2015) 171–174.
14. E. Umeshbabu, G. Rajeshkhanna, P. Justin, G.R. Rao, "Magnetic, optical and electrocatalytic properties of urchin and sheaf-like $NiCo_2O_4$ nanostructures", *Mater. Chem. Phys*., **165** (2015) 235–244.
15. G.M. Tomboc, M.W. Abebe, A.F. Baye, H. Kim, "Utilization of the superior properties of highly mesoporous PVP modified $NiCo_2O_4$ with accessible 3D nanostructure and flower-like morphology towards electrochemical methanol oxidation reaction", *J. Energy Chem*., **29** (2019) 136–146.
16. S. Smidstrup, T. Markussen, P. Vancraeyveld, J. Wellendorff, J. Schneider, T. Gunst, B. Verstichel, D. Stradi, P.A. Khomyakov, U.G. Vej-Hansen, M.-E. Lee, S.T. Chill, F. Rasmussen, G. Penazzi, F. Corsetti, A. Ojanperä, K. Jensen, M.L.N. Palsgaard, U. Martinez, A. Blom, M. Brandbyge, K. Stokbro, "QuantumATK: An integrated platform of electronic and atomic-scale modelling tools", *J. Phys. Condens. Mat.*, **32** (2019) 015901.
17. J.P. Perdew, K. Burke, M. Ernzerhof, "Generalized Gradient Approximation made simple", *Phys. Rev. Lett*., **77** (1996) 3865–3868.
18. J.P. Perdew, K. Burke, Y. Wang, "Generalized gradient approximation for the exchange-correlation hole of a many-electron system", *Phys. Rev. B*, **54** (1996) 16533–16539.
19. V. Nagarajan, R. Chandiramouli, "Adsorption ability of germanane nanosheets towards nitrogen and sulfur mustard gas molecules: A first-principles study", *J. Inorg. Organomet. Polym*., **29** (2019) 2035–2043.
20. V. Nagarajan, N. Srividya, R. Chandiramouli, "Interaction studies of liver cancer biomarkers on black phosphorene sheets – A DFT outlook", *FlatChem*., **30** (2021) 100293.
21. B. Li, J. Feng, Y. Qian, S. Xiong, "Mesoporous quasi-single-crystalline $NiCo_2O_4$ superlattice nanoribbons with optimizable lithium storage properties", *J. Mater. Chem. A*, **3** (2015) 10336–10344.
22. N. Kishore, V. Nagarajan, R. Chandiramouli, "Mechanical properties and band structure of CdSe and CdTe nanostructures at high pressure - A first-principles study", *Process. Appl. Ceram*., **13** (2019) 124–131.
23. A. Kumar, P.K. Ahluwalia, "Electronic structure of transition metal dichalcogenides monolayers 1H-MX_2 (M = Mo, W; X = S, Se, Te) from ab-initio theory: New direct band gap semiconductors", *Eur. Phys. J. B*, **85** (2012) 186.
24. A. Kumar, P.K. Ahluwalia, "Mechanical strain dependent electronic and dielectric properties of two-dimensional honeycomb structures of MoX_2 (X = S, Se, Te)", *Physica B Condens. Mat.*, **419** (2013) 66–75.
25. V. Nagarajan, R. Chandiramouli, "Acetaminophen and mepirizole molecular adsorption studies on novel χ – phosphorene nanotube based on first-principles investigation", *Mol. Simul*., **49** (2022) 99–108.
26. B. Mohan, A. Kumar, P.K. Ahluwalia, "A first principle study of interband transitions and electron energy loss in mono and bilayer graphene: Effect of external electric field", *Physica E*, **44** (2012) 1670–1674.
27. M.S. Jyothi, V. Nagarajan, R. Chandiramouli, "Cholormethane and bromomethane adsorption studies on hexstar phosphorene nanoribbon – A DFT insight", *Comput. Theor. Chem*., **1219** (2023) 113961.
28. I.T. Papadas, A. Ioakeimidis, G.S. Armatas, S.A. Choulis, "Low-temperature combustion synthesis of a spinel $NiCo_2O_4$ hole transport layer for perovskite photovoltaics", *Adv. Sci*., **5** (2018) 1701029.
29. T.-C. Chang, Y.-T. Lu, C.-H. Lee, J.K. Gupta, L.J. Hardwick, C.-C. Hu, H.-Y.T. Chen, "The effect of degrees of inversion on the electronic structure of spinel $NiCo_2O_4$: A density functional theory study", *ACS Omega*, **6** (2021) 9692–9699.
30. D. Zagorac, J. Zagorac, K. Doll, M. Cebela, B. Matovic, "Extreme pressure conditions of bas based materials: Detailed study of structural changes, band gap engineering, elastic constants and mechanical properties", *Process. Appl. Ceram*., **13** (2019) 401–410.
31. R. Yang, C. Zhu, Q. Wei, D. Zhang, "First-principles study on phases of AlP", *Solid State Commun*., **267** (2017) 23–28.
32. Q.-J. Liu, Z.-T. Liu, L.-P. Feng, B. Xu, "Electronic structure, effective masses, mechanical and thermo-acoustic properties of cubic HfO_2 under pressure", *Phys. Stat. Sol. B*, **248** (2010) 950–955.
33. N. Kishore, V. Nagarajan, R. Chandiramouli, "First-principles studies on mechanical properties and band structures of TMO_2 (TM = Zr or Hf) nanostructures under high pressure", *Physica B Condens. Mat.*, **559** (2019) 1–7.
34. H. Li, Z. Wang, G. Sun, P. Yu, W. Zhang, "First-principles study on the structural, elastic and electronic properties of Ti_2SiN under high pressure", *Solid State Commun*., **237-238** (2016) 24–27.
35. R. Yang, C. Zhu, Q. Wei, Z. Du, "Investigations on structural, elastic, thermodynamic and electronic properties of TiN, Ti_2N and Ti_3N_2 under high pressure by first-principles", *J. Phys. Chem. Solids*, **98** (2016) 10–19.
36. K. Choudhary, G. Cheon, E. Reed, F. Tavazza, "Elastic

properties of bulk and low-dimensional materials using van der Waals density functional", *Phys. Rev. B*, **98** (2018) 014107.
37. R. Ahmed, Fazal-e-Aleem, S.J. Hashemifar, H. Akbarzadeh, "First-principles study of the structural and electronic properties of III-phosphides", *Physica B Condens. Mat.*, **403** (2008) 1876–1881.
38. S.F. Pugh, "Relations between the elastic moduli and the plastic properties of polycrystalline pure metals", *The London, Edinburgh, and Dublin Philosophical Magazine and Journal of Science*, **45** (1954) 823–843.
39. G. Yi, X. Zhang, J. Qin, J. Ning, S. Zhang, M. Ma, R. Liu, "Mechanical, electronic and thermal properties of Cu_5Zr and Cu_5Hf by first-principles calculations", *J. Alloys Compd.*, **640** (2015) 455–461.
40. R. Chandiramouli, V. Nagarajan, "First-principles studies on band structure and mechanical properties of $BiFeO_3$ ceramics under high pressure", *Process. Appl. Ceram.*, **11** (2017) 120–126.
41. Y. Lu, D. Jia, F. Gao, Z. Chen, T. Hu, "First-principles study on the elastic properties of Sr-Ti-O ceramics", *Solid State Commun.*, **182** (2014) 43–46.
42. F.W. Vahldiek, S.A. Mersol, *Anisotropy in Single-Crystal Refractory Compounds*, Springer US, 1968.
43. N. Kishore, V. Nagarajan, R. Chandiramouli, "High-pressure studies on electronic and mechanical properties of $FeBO_3$ (B = Ti, Mn, Cr) ceramics – A first-principles study", *Phase Transit.*, **91** (2017) 382–397.